



1 **Into the Noddyverse: A massive data store of 3D geological models for**
2 **Machine Learning & inversion applications**

3 Mark Jessell^{1,5}; Jiateng Guo²; Yunqiang Li²; Mark Lindsay^{1,5}; Richard Scalzo^{3,5}; J r mie Giraud¹;
4 Guillaume Pirot^{1,5}; Ed Cripps^{4,5}; Vitaliy Ogarko^{1,5}

5 ¹ Mineral Exploration Cooperative Research Centre, Centre for Exploration Targeting, The University of Western Australia,
6 Perth, Australia.

7 ² College of Resources and Civil Engineering, Northeastern University, Shenyang, China.
8

9 ³ School of Mathematics and Statistics, University of Sydney, Sydney, Australia

10 ⁴ Department of Mathematics and Statistics, The University of Western Australia, Perth, Australia.

11 ⁵ ARC Centre for Data Analytics for Resources and Environments (DARE)

12

13 *Correspondence to:* Mark Jessell (mark.jessell@uwa.edu.au)

14



15 **Abstract**

16

17 Unlike some other well-known challenges such as facial recognition, where Machine Learning and Inversion algorithms are
18 widely developed, the geosciences suffer from a lack of large, labelled datasets that can be used to validate or train robust
19 Machine Learning and inversion schemes. Publicly available 3D geological models are far too restricted in both number and
20 the range of geological scenarios to serve these purposes. With reference to inverting geophysical data this problem is further
21 exacerbated as in most cases real geophysical observations result from unknown 3D geology, and synthetic test datasets are
22 often not particularly geological, nor geologically diverse. To overcome these limitations, we have used the Noddy modelling
23 platform to generate one million models, which represent the first publicly accessible massive training set for 3D geology and
24 resulting gravity and magnetic datasets. This model suite can be used to train Machine Learning systems, and to provide
25 comprehensive test suites for geophysical inversion. We describe the methodology for producing the model suite, and discuss
26 the opportunities such a model suit affords, as well as its limitations, and how we can grow and access this resource.
27



28 **1 Introduction**

29 Although it has become the focus of intense research activity in recent times, with more papers published in the five years
30 prior to 2018 than all years before that combined, Machine Learning (ML) techniques applied to geoscience problems dates
31 back to the middle of the last century (see Van der Baan and Jutten, 2000, and Dramsch, 2020, for reviews). ML methods are
32 being applied to a whole range of geological and geophysical problems, but many of these studies face common challenges
33 due to the nature of geoscientific datasets. Karpatne et al. (2017) summarise the principal challenges as follows:

- 34 i. Objects with Amorphous Boundaries- the form, structure and patterns of geoscience objects are much more
35 complex than those found in discrete spaces that ML algorithms typically deal with, consisting of both changes in
36 topology and dimensionality of geoscience objects with time.
- 37 ii. Spatio-temporal Structure- Since almost every geoscience phenomenon occurs in the realm of space and time, we
38 need to consider evolution of systems in order to understand the current state.
- 39 iii. High Dimensionality- The Earth system is incredibly complex, with a huge number of potential variables, which
40 may all impact each other, and thus many of which may have to be considered simultaneously.
- 41 iv. Heterogeneity in Space and Time- Geoscience processes are extremely variable in space and time, resulting in
42 heterogeneous datasets in terms of both sparse and clustered data. In addition, the primary evidence for a process
43 may be erased by subsequent processes.
- 44 v. Interest in Rare Phenomena- In a number of geoscience problems, we are interested in studying objects, processes,
45 and events that occur infrequently in space and time, such as ore deposit formation and earthquakes.
- 46 vi. Multi-resolution Data- Geoscience data sets are often available via different sources and at varying spatial and
47 temporal resolutions.
- 48 vii. Noise, Incompleteness, and Uncertainty in Data- Many geoscience data sets are plagued with noise and missing
49 values. In addition, we often have to deal with observational biases during data collection and interpretation.
- 50 viii. Small sample size- The number of samples in geoscience data sets is often limited in both space and time, which of
51 course is accentuated by their high dimensionality, (iii) and our interest in rare phenomena (v). In the case
52 examined in this study, the total number of publicly available 3D geological models probably numbers less than
53 10,000,000, and they are stored in a wide variety of formats rendering comparison difficult.
- 54 ix. Paucity of Ground Truth- Even though many geoscience applications involve large amounts of data, geoscience
55 problems often lack labelled samples with ground truth.

56 In this study we specifically focus on six of these challenges by providing a database of one million 3D geological models
57 and resulting gravity and magnetic fields. We address the *Spatio-temporal Structure* of the system by using a kinematic
58 modelling engine that converts a sequence of deformation events into a 3D geological model. We address *High Dimensionality*
59 by generating a very large database of possible outcomes. This represents a fundamental point of difference from many ML
60 targets such as those studying consumer preference or movie rating or facial recognition. Although of course every human
61 face is different, with few exceptions we share the same number of features (eyes, ears, noses), and these features' size and
62 relative positions only varies within small bounds. The number, geometry, composition and relative position of features in the
63 subsurface has very wide bounds and this represents a major hurdle to the application of ML to characterising 3D geology.
64 This challenge is shared by more traditional geophysical inversion approaches (Li and Oldenburg, 1998).
65 We address issues related to *Multi-resolution Data* by providing a 'controlled' dataset, at the same resolution, it offers
66 possibilities to address multi-resolution issues, by subsampling or upscaling.



67 We address *Noise, Incompleteness, and Uncertainty in Data* by providing synthetic data, we have noise and uncertainty free
68 data, or at least under control, and complete spatial coverage over the simulation domain. The models we provide can easily
69 have a structured or unstructured noise added to them and they can be subsampled to reproduce incomplete datasets.
70 We address *Small sample size* by generating one million models, which is certainly not enough to thoroughly explore the high-
71 dimensional model space; however, it illustrates the feasibility of producing large suites of models in the near-future. Modern
72 ML training sets for popular subjects such as the human face may contain tens of millions of examples (Kollias and Zafeiriou,
73 2019). A search of the Kaggle database of training datasets (<https://kaggle.com>, which contains over 63,000 distinct datasets
74 at the time of writing) only had 151 with geoscience in the keywords, and only seismic catalogues featured as geophysical
75 data. Similarly, only 59 datasets contained 3D data, and none were related to the geosciences.
76 Finally, we address the spatial and temporal *Paucity of Ground Truth* by publishing over one million models for which the
77 full 3D lithological and petrophysical distribution is provided in a labelled form for comparison with resulting gravity and
78 magnetic fields. This challenge is also faced by geophysical inversion methods. 3D geological models built using sufficient
79 data to reduce uncertainty arguably exist, but leaving aside a strict definition of uncertainty, well-constrained 3D geological
80 models are primarily restricted to restricted areas of significant economic interest, specifically sedimentary basins and mineral
81 deposits, which only represent a sub-set of possible geological scenarios. A number of studies have built simple or complex
82 synthetic models as a way to overcome these problems by providing fully defined test cases for testing processing, imaging
83 and inversion algorithms (Versteeg, 1994; Lu et al., 2011; Salem et al., 2014; Shragge et al., 2019a and b). Whilst these
84 provide valuable insights, the efforts required to build these test cases preclude the construction of large numbers of
85 significantly different models. It is easy enough to vary petrophysical properties with fixed volumes, however varying the
86 geometry, and, in particular, the topology is time consuming.
87 Recent advances in implicit modelling allow extensive geology model suites to be generated by perturbing the data inputs to
88 the model (Caumon, 2010; Cherpeau et al., 2010; Jessell et al., 2010, Wellmann et al., 2010a & b; Wellmann, and Regenauer-
89 Lieb, 2012; Lindsay et al., 2012; Lindsay et al., 2013a and b; Lindsay et al., 2014; Wellmann et al., 2014; Wellmann et al.,
90 2017, Pakyuz-Charrier et al., 2018 a & b, 2019) as part of studies that characterised 3D model uncertainty, however since they
91 use a single model as the starting point for the stochastic simulations, these works do not provide a broad exploration of the
92 range of geological geometries and relationships found in nature. Work on the automating of modelling workflows may allow
93 us to explore the model uncertainty space more efficiently (Jessell et al., 2020).
94 In this study, we have created a massive open-access resource consisting of one million three-dimensional geological models
95 using the Noddy modelling package (Jessell, 1981; Jessell & Valenta, 1996). These are provided as the input file that defines
96 the kinematics, together with the resulting voxel model and gravity and magnetic forward- modelled response. The models
97 are classified by the sequence of their deformation histories, thus addressing a temporal *Paucity of Ground Truth*. This resource
98 is provided to anyone who would like to train a ML algorithm to understand 3D geology and the resulting potential field
99 response, or to anyone wishing to test the robustness of their geophysical inversion techniques. Guo et al. (2021) used the
100 same modelling engine to produce more than three million models of a more restricted range of parameters to train a ML
101 Convolutional Neural Network system to estimate 3D geometries from magnetic images. In this study we aim to provide a
102 much broader range of possible geological scenarios as the starting point for a more general exploration of the geological
103 model space.
104 The Noddy software has been used in the past for a range of studies due to its ease in producing ‘reasonable-looking’
105 geological models with a low design or computational cost. A precursor to this study used a hundred or so manually specified
106 models as a way of training geologists in the interpretation of regional geophysical datasets by providing a range of 3D
107 geological models and their geophysical responses (Jessell, 2002). Similarly, Clark et al. (2004) developed a suite of ore
108 deposit models and their potential-field responses. The automation of model generation using Noddy was first explored using



109 a Genetic Algorithm approach to modifying parameters as a way of inverting for potential-field geophysical data, specifically
110 gravity and magnetics (Farrell et al., 1996). Wellmann et al. (2016) developed a modern Python interface to Noddy to allow
111 stochastic variations of the input parameters to be analysed in a Bayesian framework. Finally Thiele et al. (2016 a,b) used this
112 ability to investigate the sensitivity of variations in spatial and temporal relationships as a function of variations in input
113 parameters.

114

115 In this study we draw upon the ease of generating stochastic model suites to build a publicly accessible database of one million
116 3D geological models and their gravity and magnetic responses.

117 2. Model construction

118 The Noddy package (Jessell, 1981; Jessell & Valenta 1996) provides a simple framework for building generic 3D geological
119 models and calculating the resulting gravity and magnetics responses for a given set of petrophysical properties. The 3D model
120 is defined by superimposing user-defined kinematic events that represent idealised geological events, namely base stratigraphy
121 (STRAT), folds (FOLD), faults (FAULT), unconformities (UNC), dykes (DYKE), plugs (PLUG), shear zones (SHEAR-
122 ZONE) and tilts (TILT), which, can be superimposed in any order, except for STRAT, which can only occur once and has to
123 be the first event. 3D geological models are calculated by taken the current x,y,z position of a point and unravelling the
124 kinematics (using idealised displacement equations) until we get back to the time when the infinitesimal volume of rock was
125 formed, whether defined by the initial stratigraphy, or the time of formation of a stratigraphy above an unconformity, or an
126 intrusive event. In this study, we only use the resulting voxel representation of the 3D geological models, however it is possible
127 to produce iso-surface representations of the pre-deformation location of points in an implicit scheme. We have used this tool
128 as it is rapid, taking under 15s to generate 200x200x200 voxel models with both geological and geophysical representations
129 combined using an Intel(R) Xeon(R) Gold 6254 CPU @ 3.10GHz processor, and produces ‘geologically plausible’ models
130 that may occur in nature. Given that the final 3D model depends on the user’s choice of a geological history, Noddy can be
131 thought of as a kinematic, semantic, implicit modelling scheme.

132 As opposed to Wellmann et al. ((2016)), Thiele et al. (2016) and Guo et al. (. (2021), who used a python wrapper to generate
133 stochastic model suites, in this study we have modified the C code itself to simplify use by third parties, although the
134 philosophy of model generation is an extension of, but very similar to, these earlier studies.

135 Figure 1 shows one example model set for a STRAT-TILT-DYKE-UNC-FOLD history, consisting of a 3D visualisation
136 looking from the NE of the voxel model, with some units rendered transparent for clarity, the top surface of the model an EW
137 section at the northern face of the model looking from the south, a NS section on the western face of the model looking from
138 the east, and the resulting gravity and magnetic fields.

139 3. Choice of Parameters

140 In this section we describe the choices and range of values for the parameters that we have allowed to vary for our one million
141 model suite. We recognise there are other unused modes of deformation that Noddy allows that have been ignored. The
142 selection of these parameters is based on assessing the range of parameter values that will produce suites of models that we
143 believe will help and not hinder addressing the challenges cited in the introduction to this work. For example, we limited the
144 size of the plugs so that a single plug could not replace the geology of the entire volume of interest. In the discussion, we refer
145 to additional event parameters that could be activated in future studies. We limited the study to five deformation events,
146 starting with an initial horizontal stratigraphy which is always followed by tilting of the geology. The following three events



147 are drawn randomly and independently from the event list comprised of folds, faults, unconformities, dykes, plugs, shear
148 zones and tilts. The likelihood of folds, faults and shear-zones are double the other events as we found that they had a bigger
149 impact of changing the overall 3D geology, and hence we wished to sample more of these events. This means we can have
150 $7^3=343$ distinct deformation histories, although the specific parameters for each event can also vary, so the actual
151 dimensionality of the system is much higher. For clarification, the one million models are not the result of a combinatorial
152 approach, but of one million independent draws using a Monte Carlo sampling of the model space.

153 The initial stratigraphy as well as new, above-unconformity stratigraphies, are defined to randomly have between two and five
154 units to keep the systems relatively simple, but this could of course be increased if desired. The lithology of each unit in a
155 stratigraphy is chosen to be coherent with the specific event and other units in the same sequence, so that we do not, for
156 example, mix high-grade metamorphic lithologies and un-metamorphosed mudstones in the same stratigraphic series (Table
157 2) nor do we assign the petrophysical properties of a sandstone to an intrusive plug. Once a lithology is chosen, the density
158 and magnetic susceptibility is randomly sampled from a table defining the Gaussian distribution of properties (linear for
159 density, log-linear for magnetic susceptibility) for that rock type. In the case of densities this may result in occasional negative
160 values, however since the gravity field is only sensitive to density contrasts this does not invalidate the calculation. Some rock
161 types have bimodal petrophysical properties to reflect real-world empirical observations, so we draw from a Gaussian mixture
162 in these cases. The petrophysical data is drawn from aggregated statistics (mean and standard deviation of one or two peaks)
163 of the approximately 13,500 sample British Columbia petrophysical database (Geoscience BC, 2008).

164 The parameters which can be varied for each type of event, together with the range of these parameters, is shown in Table 1.
165 These parameters can be grouped in the shape, position, scale and orientation of the events, and for a five-stage deformation
166 history require the random selection of a minimum of 23 parameters for a STRAT-TILT-TILT-TILT-TILT model up to 69
167 parameters for a STRAT-TILT-UNC-UNC-UNC model where each stratigraphy has five units. Apart from the petrophysical
168 parameters, all other parameters are randomly sampled from a uniform distribution.

169 Any subset of the geology can be calculated for any sub-volume of an infinite Cartesian space using Noddy, but we limit
170 ourselves to a 4x4x4 km volume of interest in this study. Similarly, although the geology within this volume can be calculated
171 at an arbitrary resolution, we have chosen to sample it using equant 20 m voxels as this is well below the typical resolved
172 measurement scale for these types of data when collected in the field.

173

174 Geophysical forward models were calculated using a Fourier Domain formulation using reflective padding to minimise (but
175 not remove) boundary effects. The forward gravity and magnetic field calculations assume a flat top surface with a 100 m
176 sensor elevation above this surface, and the Earth's magnetic field with vertical inclination, zero declination and an intensity
177 of 50,000 nano-tesla.

178 4. Results

179 The 7^3 possible event histories produce 343 possible sequences which averages to 2915 models per sequence. Given the
180 imposed bias towards folds, faults and shear zones, and the high-probability event sequence (FAULT-SHEAR ZONE-FOLD)
181 produced 8245 models and the low-probability event sequence (UNC-TILT-PLUG) produced only 905 models, with plateaux
182 in the number of models calculated giving event sequence frequencies at around 1000, 2000, 4000 and 8000 depending on the
183 number (0,1,2,3 respectively) of events in the sequence. Together these form a “Noddyverse” of one million 3D geological
184 models and their gravity and magnetic responses. Figure 2 shows an arbitrarily selected suite of 100 models as a 10x10 grid
185 showing the top surface and two sections of the model as in Fig 1, together with the resulting gravity and magnetic fields, to
186 show the variability of the results.



187 5. Applications

188 The same logic of using millions of Noddy models was first applied by generating a massive 3D model training set and used
189 to invert real-world magnetic data (Guo et al. 2021). That study used a model suite consisting of only FOLD, FAULT and
190 TILT events, and only one of each to predict 3D geology using a Convolutional Neural Network. This approach corresponds
191 to a use case where prior geological knowledge as to the local geological history has been used to limit the model search space,
192 and formal expert elicitation could provide an important pre-cursor step to support the generation of sensible and tractable
193 problems (citations). In addition to the CNN training demonstrated by Guo et al. (2021), we can envisage three broad
194 categories of studies that could build upon the 3D model database we present here:

195 1) **Studies into the uniqueness of 3D models relative to geological event histories.** The principal question here is
196 whether any form of clustering of the geophysical fields, and perhaps the map of the surface, can recover the event
197 sequence or event parameters. Feature extraction techniques are well-known for supporting image classification
198 and clustering, so using the same principles, can we identify unique clusters of forward models from the
199 Noddyverse, and do these clusters then correspond to distinct histories? Likewise, can we train a classifier with
200 extracted features from the forward models of the gravity and magnetic responses which can then successfully
201 identify models with similar or the same histories. Three broad aspects need to be considered here: (1) the feature
202 extraction method; (2) choice of pre-processing methods for dimensionality reduction (Self Organising Maps,
203 Principal Component Analysis, Kernel-Principal Component Analysis, t-distributed Stochastic Neighbor
204 Embedding etc.) and (3) the clustering (k-means, hierarchical methods, DBSCAN /OPTICS) or classification
205 methods (random forests, support vector machines, linear classifiers).

206 A study of geophysical image variability using a simple 2D correlation or maximal information coefficient between
207 pairs of images of different histories would be illuminating. Do we have images which are the same (or at least very
208 similar and within the noise tolerance of the geophysical fields) to each other, but belong to very different histories?
209 If these exist, the ambiguity of the histories can be examined, and we then know where we would expect poor
210 performance from ML techniques which rely on easily discriminated images. The systems of equations characterising
211 geophysical inverse problems often? have a non-unique solution. In ML research, if we only use magnetic data or
212 gravity data for inversion, we will be troubled by the non-uniqueness of the solution. However, because we have both
213 gravity data and magnetic data, we can extract features from multi-source heterogeneous data at the same time, and
214 then classify or regress after feature fusion. This could greatly reduce the influence of the non-unique solution.
215 Having a large set of models will allow clustering of models accordingly to their geophysical response and identifying
216 subsets of geological models that are geophysically equivalent and cannot be distinguished using geophysical data.
217 The analysis of diversity of such subsets of models will give an estimate of the severity of non-uniqueness and allow
218 the derivation of posterior statistical indicators conditioned by geological plausibility.

219 2) **Comparison between and training of ML systems.** We see potential applications of deep learning techniques
220 (e.g., Convolutional Neural Network and Generative Adversarial Networks) where the series of models we propose
221 may also be complemented by other datasets. In this broad topic we would seek to understand which ML
222 techniques are suitable and effective in mapping geophysical data back to the geology or geological parameters.
223 We can see potential for investigating which techniques minimise the amount of data necessary to get a good
224 constraint, i.e., the model structures that most successfully capture geological expert knowledge? This could be
225 framed as an open challenge to allow different groups to use their preferred approach to the inversion problem.

226 3) **Validation of the robustness of geophysical inversion schemes.** As previously mentioned, one of the limitations
227 to validating geophysical inversion schemes is the small number of test models available, with the resulting danger



228 that the inversion parameters are tuned to the specifics of the test model, rather than being generally applicable. The
229 Noddyverse model suite allows researchers to trial their inversions against a wide range of scenarios. It will also
230 allow the examination of the validity and generality of hypotheses at the foundation of several integration and joint
231 inversion procedures. One well-known example is the underlying assumption that the underlying models vary
232 spatially in some coherent fashion (Haber and Oldenburg, 1997; Gallardo and Meju, 2003; Giraud et al., 2021).
233 The analysis of geophysically equivalent models will also enable us to estimate how significantly joint inversion or
234 interpretation can reduce the non-uniqueness of the solution, with the potential to identify families of geological
235 scenarios more suited to joint inversion than others. It is obvious that some 3D geological models will be
236 geologically more complex than others, and that some could be used for the benchmark of deterministic
237 geophysical inversion of gravity and magnetic data, but also of other geophysical techniques relying on wave
238 phenomena.

239 6. Discussion

240 In this study we have produced a ML training dataset that attempts to address four recognised limitations of applying ML to
241 geoscientific datasets, namely *Spatio-temporal Structure*, *High Dimensionality*, *Small sample size* and *Paucity of Ground*
242 *Truth*. Contrary to the current trend, the work for the generation of a comprehensive suite of geological models did not depend
243 on the appropriate training of a neural network. We relied solely on geoscientific theory and principles while remaining
244 computationally efficient. While realistic-looking suites of geological models have been generated using Generative
245 Adversarial Networks (Zhang et al., 2019), these are generally limited to a several thousands of samples, within a limited
246 range of geological scenarios.

247 6.1 Spatiotemporal Structure

248 Noddy is by design a Spatio-temporal modelling engine that uses a geological history to generate a model. Simple variations
249 in the ordering of three events following two fixed events (STRAT & TILT), even with fixed parameters quickly demonstrates
250 the important of relative time ordering to final model geometry (Fig. 3). While Noddy is limited to simple sequential events,
251 nature presents geological processes to be coeval (such as syn-depositional faulting) or partially overlapping resulting in
252 complex spatiotemporal relationships (Thiele et al., 2016a). Nonetheless, re-ordering only sequential events still produces a
253 vast array of plausible geometries, and indicates the enormity of the model space, and the necessity of efficient methods to
254 explore them.

255 6.2 High Dimensionality

256 We have limited ourselves to five deformation events in this study, and no more than five units in any one stratigraphy. These
257 decisions were based on an idea to “keep it simple” whilst simultaneously allowing a great variety of models to be built. We
258 recognise that these are somewhat arbitrary choices. We could have true randomly complex 3D histories, leading to models
259 with, for example, nine phases of folding, however the utility of over-complicating the system is not clear, and would rarely
260 or ever be discernible in natural systems. Similarly, we limited the parameter ranges of each deformation event, again on the
261 basis that the ranges chosen made models that are more interesting. For example, there did not seem much interest in having
262 folds with very large wavelengths or very low amplitudes, as they are equivalent to small translations of the geology and
263 would translate in the geophysical measurements into a regional trend that is often approximated and removed from the
264 measurements.



265 Noddy is capable of predicting continuous variations in petrophysical properties, including variably deformed magnetic
266 remanence vectors and anisotropy of susceptibility, or densities that vary away from structures to simulate alteration patterns,
267 however we decided to limit this study to simple litho-controlled petrophysics, whilst recognising the interest of studying
268 more complex discrete-continuous systems. The indexed models could also be reused with different, simpler petrophysical
269 variations, such as keeping constant values for each rock type. Each model comes with the history file used to generate the
270 model and this provides the full label for that model, so that if additional information, such as the number of units in a series
271 is considered to be important, this can be easily extracted from the file.

272 **6.3 Small sample size**

273 The total number of models sounds impressive, however once we divide that number by the 343 different event sequences,
274 we are left with between 905 and 8245 models per sequence, which whilst still large is by no means exhaustive. There is no
275 fundamental problem with building 10 or 100 million models, and if this is found to be necessary to provide useful ML training
276 datasets we can certainly do so at the expense of an increased compute time: these models were built in around a week on a
277 computer using 20 processor cores. We can also follow try to apply a metric, such as model topology, to analyse how well
278 sampled the model space is. Thiele et al. (2016b) analysed the topology of stochastically generated Noddy models and found
279 that after 100 models for small perturbations around a starting model, the number of new topologies dropped off rapidly. In
280 our case we are not making small perturbations, so we could expect to require more models before the rate of production of
281 new topologies decays, and topology is only one possible metric for comparing models.

282 **6.4 Paucity of Ground Truth**

283 The primary goal of this study was to build a large dataset to provide a wide range of possible models for use in training ML
284 systems and to test more traditional geophysical inversion systems. The models here, whilst simpler than the large test models
285 mentioned earlier, represent to our knowledge the largest suite of 3D geological models with resulting potential field data and
286 tectonic history, which has its own utility. This usage applies equally well to classical geophysical inversion codes, which
287 have traditionally been tested on only a handful of synthetic models prior to being applied to real-world data, for which there
288 is no ground truth available.

289 **6.5 Expert Elicitation**

290 To use this suite of models as the starting point for inversion of real-world datasets (as has been pioneered by Guo et al., 2021)
291 we can envisage the introduction of expert elicitation methods to meaningfully constrain the model output space while
292 acknowledging our inherent uncertainty regarding the model input space. As a probabilistic encoder of expert knowledge,
293 formal elicitation procedures (O'Hagan, 2006) have contributed greatly to physical domain sciences where complex models
294 are essential to our understanding of the underlying processes. From climatology/meteorology/oceanography (Kennedy,
295 2008), to geology and geostatistics (Walker, 2014, and Lark et al., 2015), to hydrodynamics and engineering (Astfalck et al.,
296 2018, and Astfalck et al., 2019), the central role of expert elicitation is being increasingly recognised. The complexity and
297 parameterizations of geophysical models, and the expert knowledge that resides within the geophysical community, suggests
298 this domain should be no different. It is worth noting that the choice of parameter bounds used to define the 1 million model
299 suite in this article is itself an informal expression of expert elicitation.

300

301 **6.6 Extending to the model suite**

302 In the future we may need a better representation of the “real world” 3D model space, specifically to:



- 303 • Include more parameters from Noddy, especially for parameters such as fold profile variation, alteration near structures
304 to allow petrophysical variation within units. This would help to address the Karpatne et al. (2017) challenge of *Objects*
305 *with Amorphous Boundaries*. These are capabilities that exist within Noddy but are not used in this study.
- 306 • Allow more events to increase the range of outcomes. We arbitrarily restricted ourselves to two started events (STRAT
307 and TILT) followed by three randomly chosen events, and an extension to the model suite could consider any number
308 of events in the sequence.
- 309 • Include magnetic remanence and anisotropy effects. At present we only model scalar magnetic susceptibility but the
310 Noddy modelling engine can calculate variable remanence and anisotropic magnetic susceptibility as well.
- 311 • Allow linked deformation events. At the moment every event is independently defined, however we could allow
312 parallel fault sets or dyke swarms, situations which commonly occur in nature.
- 313 • Predict different types of geophysical fields. For example, the SimPEG package (Cockett et al., 2015) could easily be
314 linked to this system to predict electrical fields (Cockett et al. 2015).
- 315 • Model larger volumes as large, or deep features cannot currently be modelled due to the 4 km model dimensions.
- 316 • Build more models. We in no way believe we have explored the range of possible models in the present model suite,
317 and if we start in include more events, or more complex event definitions, we will certainly have to generate many more
318 models, perhaps orders of magnitude more, in order to provide robust training suites and inversion scenarios.
- 319 • Add noise to the petrophysical models and/or the resulting geophysical responses. This would help to address the
320 Karpatne et al. (2017) challenge of *Noise, Incompleteness, and Uncertainty in Data*. *Incompleteness* can be addressed
321 by removing parts of the geophysical data and does not require new models to be built. Similarly, the challenge of
322 *Multi-resolution Data- Geoscience* could be addressed by subsampling parts or all of existing geophysical outputs.
- 323 • Include topographic effects. In this study, we have ignored the effect of topography on the models, although again this
324 could be included in the future, as it is supported by Noddy.

325 We also need to be clear that a model built in Noddy is not capable of predicting all geological settings, as all Noddy models
326 are plausible geology, but not all plausible geology can be modelled by Noddy. To improve this situation, we would need to
327 improve the modelling engine itself. Similarly, the logic of trying to predict geology from geophysical datasets in this study
328 is only partially fulfilled: the geometry comes from geological events sequence, but identical geometries can be produced by
329 different event sequences.

330 7. Conclusions

331 This study represents our first steps in producing geologically reasonable training sets for ML and geophysical inversion
332 applications. We have used Noddy to generate a very large, open-access 1M model, set of 3D geology and resulting gravity
333 and magnetic models as a ML training sets. These training sets can also be used as test cases for gravity and/or magnetic
334 inversions. The work presented here may be a first step to overcoming some of the fundamental limitations of applying these
335 techniques to natural geoscientific datasets.



336 8. Acknowledgements

337 We acknowledge the support from the ARC-funded Loop: Enabling Stochastic 3D Geological Modelling consortia
338 (LP170100985), DECRA (DE190100431) and Data Analytics for Resources and Environment ITTC (IC190100031). The
339 work has been supported by the Mineral Exploration Cooperative Research Centre whose activities are funded by the
340 Australian Government's Cooperative Research Centre Programme. This is MinEx CRC Document 2021/***. This work was
341 further supported by the ARC Data Analytics for Resources and Environments ITTC (IC190100031). We would like to thank
342 AARNET for supporting this work by hosting the 500GB model suite at CloudStor.
343

344 9. Code and Data availability

345

346 A doi (<https://zenodo.org/record/4589883>) provides access GitHub repository which contains the following elements
347 (Jessell, 2021):

- 348 1. The source code (C language) for the version of nobby adapted to producing random models.
- 349 2. A readme.md file with a link to the windows version of the Noddy software, plus a link to 343 tar files, one for
350 each event history ordering of the model suite.
- 351 3. A Jupyter Notebook (python code) for sampling from and unpacking the models.
- 352 4. A link in the same readme.md file to the equivalent *mybinder.org* version of the notebook so that no code
353 installation is required to sample from and view the model suite:
354 <https://mybinder.org/v2/gh/Loop3D/noddyverse/HEAD?filepath=noddyverse-remote-files-1M.ipynb>

355 All codes and data are released under the MIT licence.

356 10. Author Contribution

357 Mark Jessell wrote the original and modified nobby software, ran the experiments and wrote the python software for
358 visualising the models. Jiateng Guo and Yunqiang Li were involved in conceptualisation and manuscript preparation. Mark
359 Lindsay, Jérémie Giraud and Guillaume Pirot were involved in the conceptualisation, as well as in co-writing the introduction
360 and discussions sections of the paper. Vitaliy Ogarko, Richard Scalzo and Ed Cripps were involved in developing and co-
361 writing the introductions and discussion sections of the manuscript.

362 11. References

- 363 Astfalck, L., Cripps, E., Gosling, J.P., Hodkiewicz, M. and Milne, I.: Expert elicitation of directional metocean parameters,
364 *Ocean Engineering*. 161 pp 268-276, 2018.
- 365 Astfalck, L., Cripps, E., Gosling, J.P. and Milne, I.: Emulation of vessel motion simulators for computationally efficient
366 uncertainty quantification, *Ocean Engineering*. 172 pp 726--736, 2019.
- 367 Caumon, G.: Towards stochastic time-varying geological modeling. *Mathematical Geosciences*, 42(5), 555–569., 2010.
- 368 Cherpeau, N., Caumon, G., Caers, J., Levy, B.E.: Method for Stochastic Inverse Modeling of Fault Geometry and
369 Connectivity Using Flow Data, *Mathematical Geosciences*, 44, 147-168, 2012



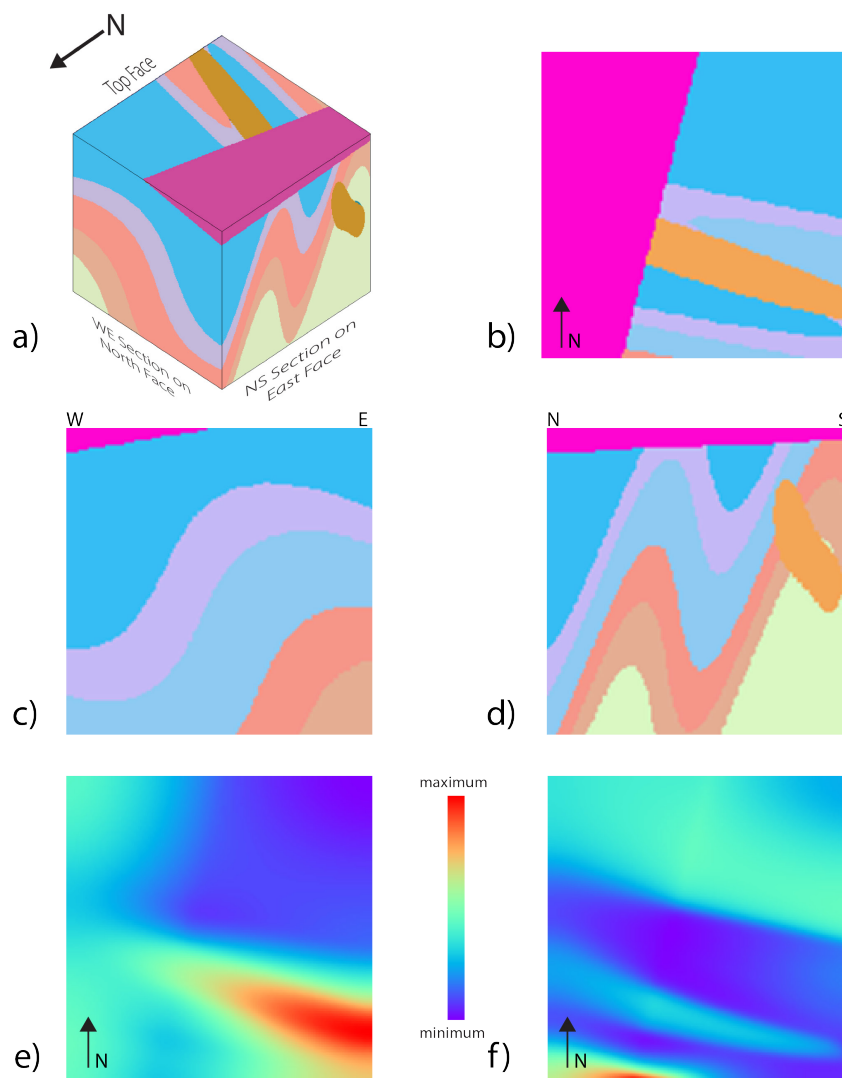
- 370 Clark, D.A., Geuna, S. and Schmidt, P.W.: 2004. Predictive magnetic exploration models for porphyry, Epithermal and iron
371 oxide copper-gold deposits: Implications for exploration. Short course manual for AMIRA p700 project available
372 at:
373 [https://confluence.csiro.au/download/attachments/26574957/Clark%20etal%202004%20P700%20CSIRO%20107](https://confluence.csiro.au/download/attachments/26574957/Clark%20etal%202004%20P700%20CSIRO%201073Rs.pdf?version=2&modificationDate=1460597746010&api=v2)
374 [3Rs.pdf?version=2&modificationDate=1460597746010&api=v2](https://confluence.csiro.au/download/attachments/26574957/Clark%20etal%202004%20P700%20CSIRO%201073Rs.pdf?version=2&modificationDate=1460597746010&api=v2)[https://confluence.csiro.au/download/attachments](https://confluence.csiro.au/download/attachments/26574957/Clark%20etal%202004%20P700%20CSIRO%201073Rs.pdf?version=2&modificationDate=1460597746010&api=v2)
375 [/26574957/Clark%20etal%202004%20P700%20CSIRO%201073Rs.pdf?version=2&modificationDate=14605977](https://confluence.csiro.au/download/attachments/26574957/Clark%20etal%202004%20P700%20CSIRO%201073Rs.pdf?version=2&modificationDate=1460597746010&api=v2)
376 [46010&api=v2](https://confluence.csiro.au/download/attachments/26574957/Clark%20etal%202004%20P700%20CSIRO%201073Rs.pdf?version=2&modificationDate=1460597746010&api=v2) , 2004.
- 377 Cockett, R., Lindsey, S.K., Heagy, J., Pidlisecky, A., Oldenburg, D.W.: 2015. SimPEG: An open-source framework for
378 simulation and gradient based parameter estimation in geophysical applications, *Computers & Geosciences*, 85, 142-
379 154, 2015.
- 380 Dramsch, J.S.: 2020. 70 years of machine learning in geoscience in review, *Advances in Geophysics*, Volume 61, 1-55, 2020.
- 381 Farrell, S. M., Jessell, M. W., Barr, T. D.: Inversion of Geological and Geophysical Data Sets Using Genetic Algorithms.
382 Society of Exploration Geophysicists Extended Abstract, 1404-1406, 1996.
- 383 Geoscience BC, : 2008. Development and Application of a Rock Property Database for British Columbia, Geoscience BC
384 Project Report 2008-9. Geoscience BC, 66 pages. Available at: [https://catalogue.data.gov.bc.ca/dataset/rock-](https://catalogue.data.gov.bc.ca/dataset/rock-properties-database)
385 [properties-database](https://catalogue.data.gov.bc.ca/dataset/rock-properties-database), 2008.<https://catalogue.data.gov.bc.ca/dataset/rock-properties-database>
- 386 Giraud, J., Ogarko, V., Martin, R., Jessell, M., Lindsay, M.: Structural, petrophysical and geological constraints in potential
387 field inversion using the Tomofast-x v1.0 open-source code, *Geoscience Model Development*, preprint.
388 <https://gmd.copernicus.org/preprints/gmd-2021-14/>, 2021.<https://gmd.copernicus.org/preprints/gmd-2021-14/>
- 389 Guo, J., Li, Y.; Jessell, M.; Giraud, J; Li, C.; Wu, L.; Li, F.; Liu, S.: 3D Geological Structure Inversion from Noddy-Generated
390 Magnetic Data Using Deep Learning Methods. *Computers and Geosciences*, 149, 104701, in press. 2021.
- 391 Jessell, 2002. M.W. An atlas of structural geophysics II. *Journal of the Virtual explorer*, 5. <http://tectonique.net/asn> , 2002..
- 392 Jessell, M. W., Ailleres, L., & Kemp, A. E.: Towards an integrated inversion of geoscientific data: What price of geology?
393 *Tectonophysics*, 490(3–4), 294–306, (2010).
- 394 Jessell, M., Ogarko, V., YohanYhan de Rose, Y., Lindsay, M., Joshi, R., Piechocka, A., Grose, L., de la Varga, M., Laurent
395 Ailleres, L., Pirot, G.: Automated geological map deconstruction for 3D model construction using map2loop 1.0 and
396 map2model 1.0, *Geoscience Model Development*, <https://doi.org/10.5194/gmd-2020-400>,
397 <https://doi.org/10.5194/gmd-2020-400>
- 398 Jessell, M.W. & Valenta, R.K.: 1996. Structural Geophysics: Integrated structural and geophysical mapping. In: *Structural*
399 *Geology and Personal Computers*, Ed. D.G. DePaor. 303-324. Elsevier Science Ltd, Oxford. 542 pp, 1996.
- 400 Jessell, M.W.: NODDY- An interactive map creation package, Unpublished MSc, University of London, 1981.
- 401 Jessell, M.W.: Loop3D/noddyverse: Noddyverse 1.0.1, <https://zenodo.org/record/4589883>, 2021.
- 402 Karpatne, A., Ebert-Uphoff, I., Ravela, S., Ali Babaie, H., Kumar, V.: Machine Learning for the Geosciences: Challenges and
403 Opportunities. *IEEE Transactions on Knowledge and Data Engineering*. DOI: 10.1109/TKDE.2018.2861006, 2017.
- 404 Kennedy, M., Anderson, C., O'Hagan, A., Lomas, M., Woodward, I., Gosling, J.P., Heinemeyer, A.: Quantifying uncertainty
405 in the biospheric carbon flux for England and Wales. *Journal of the Royal Statistical Society: Series A (Statistics in*
406 *Society)* 171, 109-135, 2008.
- 407 Kollias, D., Zafeiriou, S.: Expression, affect, action unit recognition: Aff-wild2, multi-task learning and arcfac. *British*
408 *Machine Vision Conference (BMVC)*, 2019. arXiv:1910.04855, 2019.
- 409 Lark, R., Lawley, R., Barron, A., Aldiss, D., Ambrose, K., Cooper, A., Lee, J., Waters, C.: Uncertainty in mapped geological
410 boundaries held by a national geological survey: Eliciting the geologists' tacit error model. *Solid Earth* 6, 727, 2015.
- 411 Li, Y., Oldenburg, D.W.: 1998. 3-D inversion of gravity data. *Geophysics*, 63, 109-119, 1998.



- 412 Lindsay, M. D., Jessell, M. W., Ailleres, L., Perrouty, S., de Kemp, E., & Betts, P. G.: Geodiversity: Exploration of 3D
413 geological model space. *Tectonophysics*, 594, 27–37, 2013a.
- 414 Lindsay, M. D., Perrouty, S., Jessell, M. W., & Ailleres, L.: Making the link between geological and geophysical uncertainty:
415 Geodiversity in the Ashanti Greenstone Belt. *Geophysical Journal International*, 195(2), 903–922, 2013b.
- 416 Lindsay, M., Ailleres, L., Jessell, M. W., de Kemp, E., & Betts, P. G.: Locating and quantifying geological uncertainty in
417 three-dimensional models: Analysis of the Gippsland Basin, Southeastern Australia. *Tectonophysics*, 546-547, 10–
418 27, 2012.
- 419 Lindsay, M., Perrouty, S., Jessell, M. W., & Ailleres, L.: Inversion and geodiversity: Searching model space for the answers.
420 *Mathematical Geosciences*, 46(8), 971–1010, 2014.
- 421 Lu, S., Whitmore, N.D., Valenciano, A.A. Chemingui, N., 2011: Imaging of primaries and multiples with 3D SEAM synthetic,
422 SEG Technical Program Expanded Abstracts: 3217-3221, 2011.
- 423 O'Hagan, A., Buck, C.E., Daneshkhah, A., Eiser, J.R., Garthwaite, P.H., Jenkinson, D.J., Oakley, J.E., Rakow, T.: Uncertain
424 judgements: Eliciting experts' probabilities. John Wiley & Sons, 2006.
- 425 Pakyuz-Charrier E, Giraud J, Ogarko V, Lindsay, M., and Jessell, M.: Drillhole uncertainty propagation for three-dimensional
426 geological modelling using Monte Carlo. *Tectonophysics*. doi: 10.1016/j.tecto.2018.09.005, 2018a.
- 427 Pakyuz-Charrier, E., Jessell, M., Giraud, J., Lindsay, M. & Ogarko, V.: Topological analysis in Monte Carlo simulation for
428 uncertainty propagation, *Solid Earth*. 10, 1663-1684, 2019.
- 429 Pakyuz-Charrier, E., Lindsay, M., Ogarko, V., Giraud, J., and Jessell, M.: Monte Carlo simulation for uncertainty estimation
430 on structural data in implicit 3-D geological modelling, a guide for disturbance distribution selection and
431 parameterization, *Solid Earth*, 9, 385–402, <https://doi.org/10.5194/se-9-385-2018>, 2018b.
- 432 Salem, A., Green, C., Cheyney, C., Fairhead, J.D., Aboud, E., Campbell, S.: Mapping the depth to magnetic basement using
433 inversion of pseudogravity, application to the Bishop model and the Stord Basin, northern North Sea, *Interpretation*
434 2, 1M-T127, 2014.
- 435 Shragge, J., Bourget, J., Lumley, D., Giraud, J.: The Western Australia Modeling (WAMo) Project. Part I: Geomodel Building.
436 *Interpretation* 7(4):1-67, 2019a.
- 437 Shragge, J., Lumley, D., Bourget, J., Potter, T., Miyoshi, T., Witten, B., Giraud, J., Wilson, T., Iqbal, A., Emami Niri, M.,
438 Whitney, B.: The Western Australia Modeling (WAMo) Project. Part 2: Seismic Validation. *Interpretation*, 7(4), 1-
439 62, 2019b.
- 440 Thiele, S.T., Jessell, M.W., Lindsay, M. Ogarko, V., Wellmann, F., Pakyuz-Charrier, E.: The Topology of Geology 1:
441 Topological Analysis. *Journal of Structural Geology*, 91, 27-38, 2016a.
- 442 Thiele, S.T., Jessell, M.W., Lindsay, M., Wellmann, F., Pakyuz-Charrier, E. 2016b.: The Topology of Geology 2: Topological
443 Uncertainty. *Journal of Structural Geology*, 91, 74-87, 2016b.
- 444 Van der Baan, M., Jutten, C.: Neural networks in geophysical applications. *Geophysics*, 65, 1032-1047, 2000.
- 445 Versteeg, R.: The Marmousi experience: Velocity model determination on a synthetic complex data set. *The Leading Edge*,
446 September 1994, 927-936, 1994.
- 447 Walker, M., and Curtis, A.: “Eliciting spatial statistics from geological experts using genetic algorithms.” *Geophysical Journal*
448 *International*, Volume 198, Issue 1, Pages 342-356, <https://doi.org/10.1093/gji/ggu132>, 2014.
- 449 Wellmann, F., & Regenauer-Lieb, K.: Uncertainties have a meaning: Information entropy as a quality measure for 3-D
450 geological models. *Tectonophysics*, 526, 207–216, 2012.
- 451 Wellmann, F., de la Varga, M., Murdie, R. E., Gessner, K., & Jessell, M. W.: Uncertainty estimation for a geological model
452 of the Sandstone greenstone belt, Western Australia—Insights from integrated geological and geophysical inversion
453 in a Bayesian inference framework. *Geological Society, London, Special Publications*, 453, 41–52, 2017.



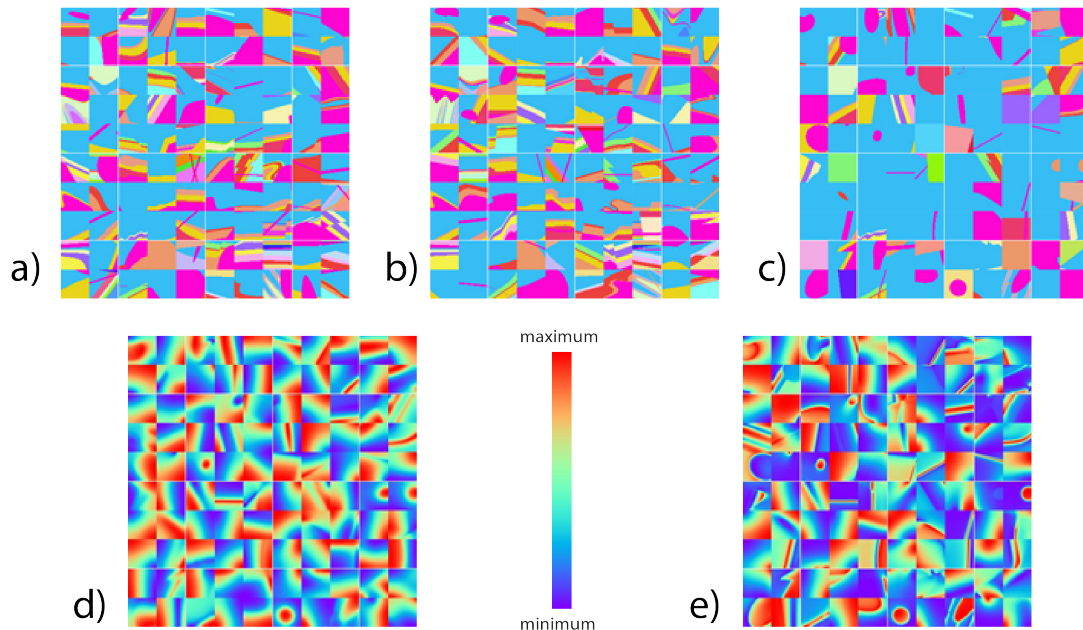
- 454 Wellmann, F., Horowitz, F. G., Schill, E., & Regenauer-Lieb, K.: Towards incorporating uncertainty of structural data in 3D
455 geological inversion. *Tectonophysics*, 490(3–4), 141–151, 2010b.
- 456 Wellmann, F., Horowitz, F. G., Schill, E., & Regenauer-Lieb, K.: Towards incorporating uncertainty of structural data in 3D
457 geological inversion. *Tectonophysics*, 490(3–4), 141–151, 2010a.
- 458 Wellmann, J.F., Lindsay, M., Poh, J., Jessell, M.: Validating 3-D Structural Models with Geological Knowledge for
459 meaningful Uncertainty Evaluations. *Energy Procedia*, 59, 374-381, 2014.
- 460 Wellmann, J.F., Thiele, S., Lindsay, M., Jessell, M.W.: pynoddy: An Experimental Platform for Automated 3D Kinematic
461 and Potential Field Modelling. *Geoscientific Model Development*. 9, 1019-1035. doi: :10.5194/gmd-9-1019-2016,
462 2016.
- 463 Zhang, T.-F., Tilke, P., Dupont, E., Zhu, L.-C., Liang, L., Bailey, W.: Generating geologically realistic 3D reservoir facies
464 models using deep learning of sedimentary architecture with generative adversarial networks. *Petroleum Science*,
465 16, 541–549, 2019.
- 466
- 467
- 468
- 469



470

471 **Figure 1.** Example model set for a STRAT-TILT-DYKE-UNC-FOLD sequence showing a) 3D visualisation looking from the NE of
472 the voxel model, b) the top surface of the model, c) an EW section at the northern face of the model looking from the south, d) a NS
473 section on the western face of the model looking from the west, and the resulting e) gravity and f) magnetic fields. Geophysical
474 images are all normalized to model max-min values.

475



476

477

478

479

480

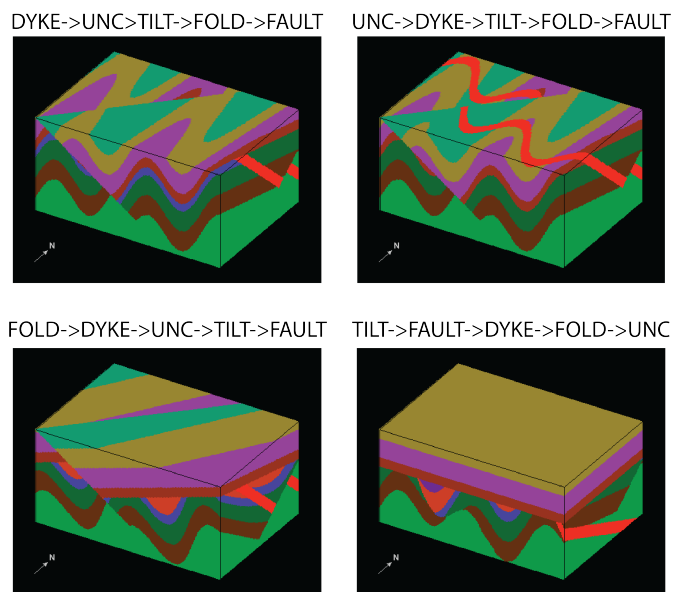
481

482

Figure 2. Example models for 100 randomly selected models drawn from the 1M model suite showing a) the top surface of the model, b) an EW section at the northern face of the model looking from the south, c) a NS section on the western face of the model looking from the west, and the resulting d) gravity and e) magnetic fields. Geophysical images are all normalized to model max-min values.



483



484

485

486

Figure 3. Four possible 3D geological models with the same base stratigraphy (STRAT) followed by five events using four of the possible different event ordering sequences.



487
488

Event type	Parameter 1	Parameter 2	Parameter 3	Parameter 4	Parameter 5	Parameter 6	Min/Max number of parameters
Base Stratigraphy	Number of units. Range: 2-5	unit n thickness: 50-1000 m	Density of each unit: depends on lithology of unit n	Magnetic susceptibility of each unit: depends on lithology of unit n			5/12
Fold	Wavelength : 1,000-11,000 m	Amplitude : 200 - 5,000 m	Azimuth : 0-360 degrees	Inclination : 0-90 degrees	Phase : 0-4000 m	Along axis amplitude decay : 500-9,500 m	6/6
Fault	Position of l point on fault: x,y,z 2000-4000 m	Displacement : 0-2000 m	Azimuth : 0-360 degrees	Inclination : 0-90 degrees	Pitch of displacement : 0-90 degrees		7/7
Unconformity	Position of l point on Unconformity: x=2000-3000m y=2000-4000m z=3000-4000 m	Number of units above unconformity: 2-5	Azimuth : 0-360 degrees	Inclination : 0-90 degrees	Density of each unit: depends on lithology of unit n	Magnetic susceptibility of each unit: depends on lithology of unit n	10/17
Dyke	Position of l point on fault: x=0-4000 m y=0-4000 m z=0-4000 m	Azimuth : 0-360 degrees	Inclination : 0-90 degrees	Width of Dyke : 100-400 m	Density : depends on lithology	Magnetic susceptibility : depends on lithology	8/8
Plug	Shape : Cylindrical, Conic, Parabolic, Ellipsoidal	Position of centre of plug: x=1000-4000m y=1000-4000m z=1000-4000m	Size of plug: parameter varies with shape	Density : depends on lithology	Magnetic susceptibility : depends on lithology		7/9
Tilt	Position of l point on rotation axis: x=2000-3000m y=2000-4000m z=3000-4000 m	Azimuth : 0-360 degrees	Inclination : 0-90 degrees	Rotation : -90-90 degrees			6/6
Shear zone	Position of l point on fault: x,y,z 2000-4000 m	Displacement : 0-2000 m	Azimuth : 0-360 degrees	Inclination : 0-90 degrees	Pitch of displacement : 0-90 degrees	Width of Shear Zone : 100-2000 m	8/8

Table 1. Free parameters with their allowable ranges for each event.



489

Lithology	Lithology Class	Genetic Class	Mean Density g.cm-3	Standard Deviation Density	Mean Log Susceptibility (cgs)	Standard Deviation Log Susceptibility	Susceptibility Bimodality Flag
Felsic Dyke Sill	Dyke	Intrusive	2.612593	0.090526329	-3.693262	1.50094258	1
Mafic Dyke Sill	Dyke	Intrusive	2.793914	0.015759637	-2.119223	0.85376583	0
Granite	Plug	Intrusive	2.691577	0.094589692	-2.455842	0.86575449	1
Peridotite	Plug	Intrusive	2.851076	0.154478049	-1.158807	0.4390425	0
Porphyry	Plug	Intrusive	2.840024	0.128971814	-2.613833	0.99194475	1
Pyxenite Hbndite	Plug	Intrusive	3.194379	0.253322535	-1.946615	1.03641373	0
Gabbro	Plug	Intrusive	3.004335	0.159718751	-2.124022	0.82126305	1
Diorite	Plug	Intrusive	2.851608	0.134656746	-2.088111	0.81829275	1
Syenite	Plug	Intrusive	2.685824	0.115078068	-2.461453	0.91295395	1
Amphibolite	Met strat	Metamorphic	2.875933	0.142164171	-2.69082	0.90733619	1
Gneiss	Met strat	Metamorphic	2.701191	0.073583537	-3.18094	0.95259725	1
Marble	Met strat	Metamorphic	2.871775	0.532997473	-3.671996	1.25374051	0
Meta Carbonate	Met strat	Metamorphic	2.738965	0.036720136	-3.117868	0.82945531	0
Meta Felsic	Met strat	Metamorphic	2.782584	0.301451931	-3.55755	0.65748564	1
Meta Intermediate	Met strat	Metamorphic	2.894892	0.265153614	-3.673276	0.26107008	0
Meta Mafic	Met strat	Metamorphic	2.814461	0.096381942	-3.250044	0.62513286	0
Meta Sediment	Met strat	Metamorphic	2.982992	0.49439556	-3.402807	0.89505466	1
Meta Ultramafic	Met strat	Metamorphic	2.843941	0.138208079	-2.166206	0.76543947	0
Schist	Met strat	Metamorphic	2.81978	0.109752597	-3.18525	0.69584686	0
Andesite	Met strat	Volcanic	2.721189	0.091639014	-2.15826	0.71678329	0
Basalt	Met strat	Volcanic	2.79269	0.155153198	-2.155728	0.64718503	0
Dacite	Met strat	Volcanic	2.62127	0.129131224	-2.562422	0.8166926	0
Ign V Breccia	Met strat	Volcanic	2.910459	0.101746428	-2.706956	0.73116944	0
Rhyolite	Met strat	Volcanic	2.630833	0.071233818	-3.046728	0.78711701	0
Tuff Lapillistone	Met strat	Volcanic	2.64447	0.110173772	-2.878701	0.86889142	0
V Breccia	Met strat	Volcanic	2.771579	0.167796457	-2.524945	0.90943985	0
V Conglomerate	Met strat	Volcanic	2.755267	0.10388303	-2.304483	1.00991116	0
V Sandstone	Met strat	Volcanic	2.779715	0.101133121	-2.903361	0.82701019	0
V Siltstone	Met strat	Volcanic	2.859347	0.102741619	-2.769054	0.87771183	0
Conglomerate	Strat	Sedimentary	2.618695	0.116158268	-3.31026	0.9740717	0
Limestone	Strat	Sedimentary	2.713912	0.147683486	-4.256256	0.87772406	0
Pelite	Strat	Sedimentary	2.698554	0.021464631	-3.369295	0.5295974	1
Phyllite	Strat	Sedimentary	2.739177	0.173374383	-3.696455	0.73955588	0
Sandstone	Strat	Sedimentary	2.622672	0.107003083	-3.452758	0.64521521	0
Greywacke	Strat	Sedimentary	2.861463	0.16024622	-3.841047	1.14724626	1

490

491 Table 2. Simplified petrophysical values derived from British Columbia database (Geoscience BC, 2008). Values are randomly
 492 sampled from Gaussian distributions defined by mean and standard deviation of density and log magnetic susceptibility. For
 493 lithologies with bimodal magnetic susceptibilities (flag=1), mixed sampling is based on offsetting the means by +/-0.75 orders of
 494 magnitude, which approximates the variations seen in nature.